Solid State Communications 152 (2012) 968–973

Contents lists available at SciVerse ScienceDirect

Solid State Communications

journal homepage: www.elsevier.com/locate/ssc

Investigation of possible half-metal material on double perovskites Sr_2BBO_6 (B, B=3d transition metal) using first-principle calculations

Y.P. Liu [a], S.H. Chen [b], J.C. Tung [c], Y.K. Wang [a,d,*]

[a] Department of Physics, National Taiwan Normal University, Taipei 106, Taiwan
[b] Institute of Physics, Academia Sinica, Taipei 106, Taiwan
[c] Graduate Institute of Applied Physics, National Chengchi University, Taipei 11605, Taiwan
[d] Center of General Eduaction and Department of Physics, National Taiwan Normal University, Taipei 106, Taiwan

ARTICLE INFO

Article history:
Received 13 December 2011
Accepted 20 January 2012
by A. Lichtenstein
Available online 30 March 2012

Keywords:
A. Half-metal materials
C. Double perovskites
E. First-principle calculations

ABSTRACT

We investigated the possible candidates of half-metal (HM) material in double perovskites structure $Sr_2BB'O_6$ (B, B'=3d transition metal). The electronic structure calculations were based on density functional theory (DFT) with both generalized gradient approximation (GGA) and GGA+U approaches, where +U is on-site Coulomb interaction correction. With the consideration of 4 types of magnetic states, i.e. ferromagnetic (FM), ferromagnetic (FiM), antimagnetic (AF) and nonmagnetic (NM), we found 5 promising candidates for half-metallic (HM) materials: Sr_2ScCrO_6, Sr_2TiCrO_6, Sr_2MnCrO_6, Sr_2ZnMnO_6 and Sr_2ZnFeO_6.

1. Introduction

The interest in double perovskites started with the discovery of the room-temperature colossal magnetoresistance (CMR) in Sr_2FeMoO_6 [1], which is a half-metallic (HM) material. In HM, materials are characterized by the coexistence of metallic behavior from one spin and insulating behavior from the other. Therefore, the HM materials have three characteristic properties: (1) quantization of the magnetic moment, (2) 100% spin polarization at the Fermi level, and (3) spin susceptibility of zero. Thus, the HM materials offer potential technological applications such as computer memory, magnetic recording, single-spin electron source, and high-efficiency magnetic sensors [2–4]. Therefore, the searching for half-metallic compounds is a very hot topic. HM materials include spinel Fe_3O_4 [5], rutile CrO_2 [6], double perovskites Sr_2FeMoO_6 [1], La_2VTcO_6, La_2VCuO_6 [7], spinel $FeCr_2S_4$ [8], and Mn-doping GaAs [9,10].

In ordered double perovskites noted as $A_2BB'O_6$ (A=alkaline-earth or rare-earth element, B and B'=transition metals), the differences of size and the valance between the B and B' ions are crucial for controlling the physical properties [11,12]. There are some possible HM material candidates in $Sr_2BB'O_6$ double perovskites structure from the previous study: Sr_2MnMoO_6 [13], Sr_2CuOsO_6 [14], Sr_2VOsO_6 [15], Sr_2NiRuO_6 [16], Sr_2FeTiO_6 [17], Sr_2CrMoO_6 [18,19], Sr_2CoMoO_6 [19], Sr_2CrReO_6 [20,21], Sr_2FeReO_6 [21,22], and Sr_2CrWO_6 [22,23]. In this work, we performed the calculation of $Sr_2BB'O_6$ (B, B'=3d transition metals) for 45 combinational possibilities based on the first-principle calculation with full-structure optimization by generalized gradient approximation (GGA) and consideration of strong correlation effect (GGA+U). It was found that Sr_2ScCrO_6 and Sr_2TiCrO_6 are half-metallic ferromagnets (HM–FM) and Sr_2CrMnO_6, Sr_2ZnMnO_6 and Sr_2ZnFeO_6 are half-metallic ferrimagnets (HM–FiM). The double exchange interaction is the main cause of the HM properties.

2. Computational method

The theoretical calculations were based on the first-principle density functional theory (DFT) [24]. In the structural optimization calculation (i.e., relaxation for both lattice constants and atomic positions), the full-potential projector augmented wave (PAW) [25] method was used and the generalized gradient approximation (GGA) [26], which is implemented in the VASP code [27,28] to calculate the electronic structures. The cutoff energy of the plane wave basis was set to be 450 eV, and $8\times8\times6$ k-points grids were set in the Brillouin zone. For finding the stable ionic positions, the conjugate-gradient method was used, and the energy convergence criteria for electronic self-consistent calculations were all set to 10^{-6} eV. The theoretical equilibrium structures were obtained when forces and stress acting on all the atoms were less than 0.03 eV/Å and 0.9 kbar, respectively. The

* Corresponding author at: Center of General Eduaction, National Taiwan Normal University, Taipei 106, Taiwan.
E-mail address: kant@ntnu.edu.tw (Y.K. Wang).

0038-1098/$ - see front matter © 2012 Elsevier Ltd. All rights reserved.
http://dx.doi.org/10.1016/j.ssc.2012.01.051

Table 1
Calculated physical properties of the possible FM/FiM–HM materials in double perovskite ($Sr_2BB'O_6$) structure in the full structural optimization calculation of GGA($+U$).

Materials, $Sr_2[BB']O_6$	$U(B,B')$	Spin magnetic moment (μ_B/f.u.)			d Orbital electrons↑/↓		$N(E_F)$ states (eV/f.u.)	Band gap (eV)	ΔE=FM−AF (meV)
		m_B	m'_B	m_{tot}	B	B'			
ScCr	(0,0)	0.026	1.039	1.000	0.930/0.898	2.641/1.620	↑4.720	↓1.075	−180.9
	(2,3)	0.030	1.333	1.000	0.989/0.865	2.771/1.464	↑4.384	↓1.800	−8.3
TiCr	(0,0)	0.084	1.858	2.000	1.383/1.287	3.049/1.219	↑4.162	↓1.475	−99.0
	(2,3)	0.069	2.105	2.000	1.334/1.268	3.157/1.087	↑3.931	↓2.050	−26.6
ZnNi	(0,0)	0.014	0.224	2.000	4.951/4.920	4.188/3.691	↓13.348	↑0.350	−248.8
	(7,6)	0.000	0.000	0.000	5.020/5.020	4.148/4.148	↑8.711/↓8.711		−6.6
ZnFe	(0,0)	−0.016	2.309	4.000	4.947/4.946	4.172/1.876	↓5.938	↑0.800	−65.6
	(7,5)	−0.034	2.745	4.000	5.007/5.029	4.367/1.639	↓3.340	↑0.200	−23.1
ZnMn	(0,0)	−0.035	1.628	1.000	4.932/4.970	3.232/1.621	↑5.161	↓0.900	−171.2
	(7,5)	−0.037	2.925	1.000	5.000/5.042	3.892/1.002	↑7.881	↓3.600	−85.6
MnCr	(0,0)	−2.410	1.739	−1.000	1.260/3.637	2.997/1.305	↑3.631	↓0.675	−669.4
	(5,3)	−2.796	2.146	−1.000	1.017/3.777	3.183/1.094	↑3.920	↓0.975	−231.20
ScCo	(0,0)	−0.063	1.157	2.000	0.913/0.953	4.114/2.960	↓5.799	↑1.100	−177.7
	(2,6)	0.130	3.141	4.617	0.954/0.874	5.036/1.904	↑2.463/↓2.408		20.2
TiCo	(0,0)	−0.059	0.707	1.000	1.332/1.375	3.923/3.218	↓5.187	↑0.700	−125.2
	(2,6)	0.177	3.389	5.000	1.358/1.282	5.153/1.777	↑↓0.000	↑↓2.975/0.075	4.8

Wigner–Seitz radius of the atom was set to 2.5 a.u. for Sr, to 2.1 a.u. for 3*d* materials, and to 1.4 a.u. for O.

GGA calculations were not good enough to describe strong electron correlation systems such as transition metal oxides. The deficiency in first-principle calculation was corrected by using a strong-correlation correction to the LDA of GGA, which is called the LDA(GGA)+U method [29,30]. This LDA(GGA)+U scheme, yielding quite satisfying results for many strongly correlated systems, is considered to be a useful approach [31–33]. Therefore, to see the effect of the on-site electron correlations on the half-metallic of the materials, the GGA+U calculations were performed in this work. The effective parameter $U_{eff}=U-J$ was adopted, where U and J stand for Coulumb and exchange parameters, respectively. (We will use U instead of U_{eff} for simplicity in this paper.) In 3*d* transition metals, we selected the near-maximum values from the reasonable range of U [34]. For example, the range U for Fe is 3.0–6.0 eV and 5.0 is used in the calculation. The detail U values are listed in Table 1. In ordered double perovskite structure $Sr_2BB'O_6$ (Fig. 1), four magnetic phases—ferromagnetic (FM), ferromagnetic (FiM), antimagnetic (AF) and nonmagnetic (NM)—exist and are controlled by the spin state of the two B and B' ions.

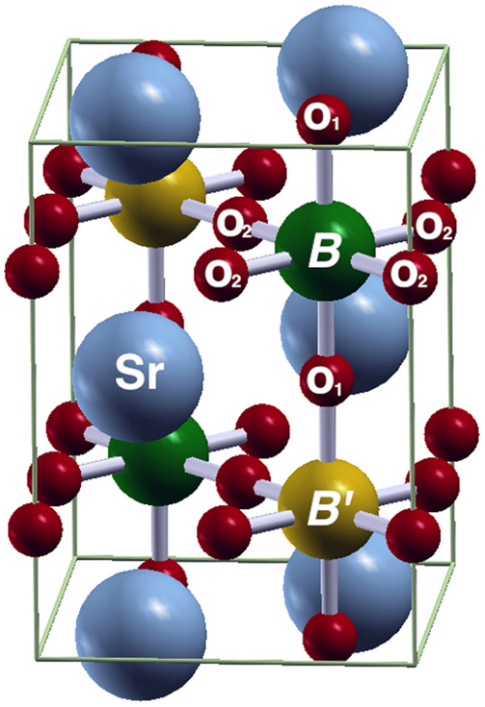

Fig. 1. (Colour online) An ideal ordered double perovskite structure $Sr_2BB'O_6$. For FiM state, the spin state of (B, B, B', B') is (+, +, −, −). For AF state, the spin state of (B, B, B', B') is (+, −, +, −).

3. Results and discussions

3.1. Crystal structures and magnetic stable phase

During full structural optimization, the ideal cubic perovskite structure ($Fm\bar{3}m$, no. 225) will reduce to tetragonal structure ($I4/mmm$, no. 139) in the FM or FiM state. In the AF state, the tetragonal structure ($P4/mmm$, no. 123) remains the same. In the ideal cubic double perovskite structure ($Fm\bar{3}m$), the B and B' ions are in the order of NaCl configuration; it can be described by a face-centered cubic (fcc) lattice with lattice constant 2*a*. Each $B(B')$ is coordinated by $B'(B)$, and each has an O ion between, so there are 6 B–O–B' bonds per unit cell with the length of B–O and B'–O being equal. After the full structural optimization, the structure will reduce from cubic (space group $Fm\bar{3}m$) to tetragonal (space group $I4/mmm$) with two nonequivalent types of O atoms shown in Table 2. There are two O_1 atoms located on the *z*-axis with B and B' atoms sitting between, and the four O_2 atoms being located on the same plane as the B and B' atoms (see Fig. 1 and Table 2). Although the lattice constant and bond length had changed after the full structural optimization, the angle of the B–O–B' remained 180°. It is shown that the symmetry reduction is rather minor, i.e., the c/a ratio being very close to the ideal value $\sqrt{2}$.

Most important, the same B and B' ions have the same spin state; that is, (B, B, B', B') =(m, m, m', m')=FM or (m, m, $-m'$, $-m'$)=FiM, which can lead us to the assumption of HM state. In the AF state, the spin state is (B, B, B', B') is (m, $-m$, m', $-m'$). In this state, there will be no half-metallic state because the total DOS of spin-up and spin-down is symmetrical, which results from the induced equivalence in the charges: $Q\uparrow[B(B')]=Q\downarrow[B(B')]$. For the NM state, there is no spin-polarized calculation, resulting in no

magnet properties. In order to know which magnetic phase is most stable, we perform the calculation for all four magnetic phases. The FM and FiM initial state always converges to only one of the state during the self-consistent process, except Sr_2MnCrO_6. The calculated results show that the total energies *with* spin polarization are always lower than that *without* spin polarization. To guarantee the accuracy of the calculation results, full structural optimization with higher convergence criteria was also performed.

In the calculation of $Sr_2 3d 3d' O_6$ series (45 compounds), there are still 14 possible HM materials during the self-consistent process in the ideal cubic double perovskite structure ($Fm\bar{3}m$, no. 225, lattice constant a=7.8 Å). After the full structural optimization calculation, the favored crystal structure of the FM/FiM state is tetragonal structure ($I4/mmm$, no. 139), and there are 9 possible HM materials left. Later, we compared the total energies among the four magnetic states; there are 8 possible FM/FiM–HM surviving stable materials, with three containing 3 FM–HM materials—Sr_2ScCrO_6, Sr_2TiCrO_6, and Sr_2ZnNiO_6—and 5 containing FiM–HM materials—Sr_2ScCoO_6, Sr_2TiCoO_6, Sr_2MnCrO_6, Sr_2ZnMnO_6 and Sr_2ZnFeO_6. For transition metals, the strong-correlation correction (GGA+U) scheme must be considered for the d orbitals with the U values noted as (U_B, $U_{B'}$). While the strong-correlation correction (GGA+U) is considered, Sr_2ZnNiO_6 falls in the NM state; Sr_2ScCoO_6 becomes metal; and Sr_2TiCoO_6 becomes insulator. Thus, this paper will focus on the 5 possible candidates of FM/FiM–HM materials.

During the self-consistent process and structural optimization, the FM and FiM of Sr_2MnCrO_6 do not converge to each other; that is, there are three magnetic states (FM, FiM and AF) existing with only one stable ground state. The FiM state is more stable than the FM state by 824.2 meV while it is also lower than the AF state by 669.4 meV; that is, the FiM state is the ground state for Sr_2MnCrO_6. Even having the consideration of strong-correlation correction, the FiM state is still the ground state by 422.9 meV for the energy difference of FM state and by 231.2 meV for the energy difference of AF state.

Table 2
Structural parameters of the possible FM/FiM–HM materials in the fully optimized structure ($I4/mmm$, no. 139) where Sr(x,y,z)=(0,0.5,0.75), B(x,y,z)=(0,0,0) and B'(x,y,z)=(0,0,0.5).

$Sr_2[BB']O_6$	ScCr	TiCr	ZnFe	ZnMn	MnCr
a	5.5735	5.4990	5.5192	5.5131	5.4105
c/a	1.4142	1.4141	1.4156	1.4145	1.4126
V_0 (Å^3/f.u.)	122.42	117.57	118.99	118.51	111.86
O_1x	0	0	0	0	0
O_1y	0	0	0	0	0
O_1z	0.2621	0.2537	0.2617	0.2620	0.2500
O_2x	0.2376	0.2470	0.2385	0.2382	0.2501
O_2y	0.2376	0.2470	0.2385	0.2382	0.2501
O_2z	0.5	0.5	0.5	0.5	0.5

4. FM–HM compounds: Sr_2ScCrO_6 and Sr_2TiCrO_6

In our study, both Sr_2ScCrO_6 and Sr_2TiCrO_6 show that the FiM state converges to the FM state after structural optimization. Therefore, the density of states (DOS) are presented in FM sate (Fig. 2). In GGA(+U) calculation, Sr_2ScCrO_6 is half-metallic with total magnetic moment 1.0μ_B and energy gap 1.08 eV at the spin-down channel. The hybridization between the Cr 3d and O 2p orbital occurs mainly in the energy region −5.5 eV to −3.5 eV and −3 eV to 1.5 eV, especially near the Fermi level (E_F) with a spin-splitting causing the HM property. And with the double exchange interaction, the O 2p and Sc 3d orbital hybrid interacts at the same energy region, which gives Sc a weak magnetic moment 0.026μ_B caused by the asymmetric of the Cr e_g at the Fermi level. The total electron numbers of d orbital for Sc and Cr are 1.83 and 4.26, respectively. This gives the valence states of $Sc^{+1.17}(3d^{1.83})$ and $Cr^{+1.74}(3d^{4.26})$. The election configuration is $Sc^{+}(3d^2)$, S=0; $Cr^{+}(3d^5)$, S=1/2 for Sr_2ScCrO_6 according to the calculated electron numbers.

For Sr_2TiCrO_6, this compound is very similar to Sr_2ScCrO_6 in many ways. It appears half-metallic with total magnetic moment 2.0μ_B and energy gap 1.45(2.1) eV in GGA(+U) process. The double exchange interaction of Cr_{3d}–O_{2p}–Ti_{3d} orbitals causes the hybridization in the energy of −6.0 eV to −1.5 eV and −0.9 eV to 2.0 eV

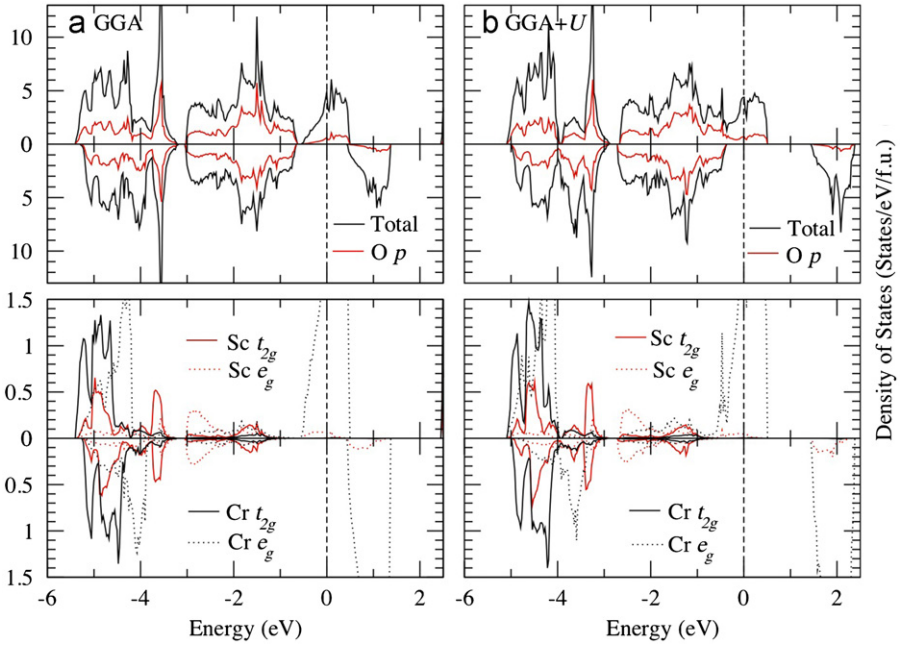

Fig. 2. (Colour online) Calculated total, spin and site decomposed density of states of Sr_2ScCrO_6: (a) GGA and (b) GGA+U(2,3).

(Fig. 3) giving Ti a small magnetic moment 0.08μ_B. The total electron numbers of d orbital for Ti and Cr are 2.67 and 4.62, respectively. This gives the valence states of $Ti^{+1.33}(3d^{2.67})$ and $Cr^{+1.38}(3d^{4.62})$. The election configuration is $Ti^{2+}(3d^2)$, $S=0$; $Cr^{+2}(3d^4)$, $S=1$ for Sr_2TiCrO_6 according to the calculated electron numbers.

From the GGA+U calculation, it can be observed that both Sr_2ScCrO_6 and Sr_2TiCrO_6 near the Fermi level, due to the electron correlation effect, moving the Sc(Ti) 3d orbital to a lower energy region. Yet it still crosses the Fermi energy level at the spin-up channel; for the spin-down channel, it only gives a wider energy gap. Thus, the strong-correlation correction changes no features of the magnetic phases, magnetic moment, and spin-conductivity.

5. FiM–HM compounds: Sr_2ZnFeO_6, Sr_2ZnMnO_6 and Sr_2MnCrO_6

In the research, FM and FiM state all converge to FiM state in structural optimization for Sr_2ZnFeO_6, Sr_2ZnMnO_6 and Sr_2MnCrO_6. Therefore, the density of states (DOS) is presented in FiM sate (Figs. 4–6). For Sr_2ZnFeO_6, half-metallic properties are obtained with total magnetic moment 4.0μ_B and energy gap 0.80 eV during the GGA calculations. While considering the electron correlation effect, the Fe t_{2g} orbital at spin-down channel lifts and e_g at spin-up channel becomes closer to E_F causing the energy gap to narrow from 0.80 eV to 0.20 eV. The energy split of

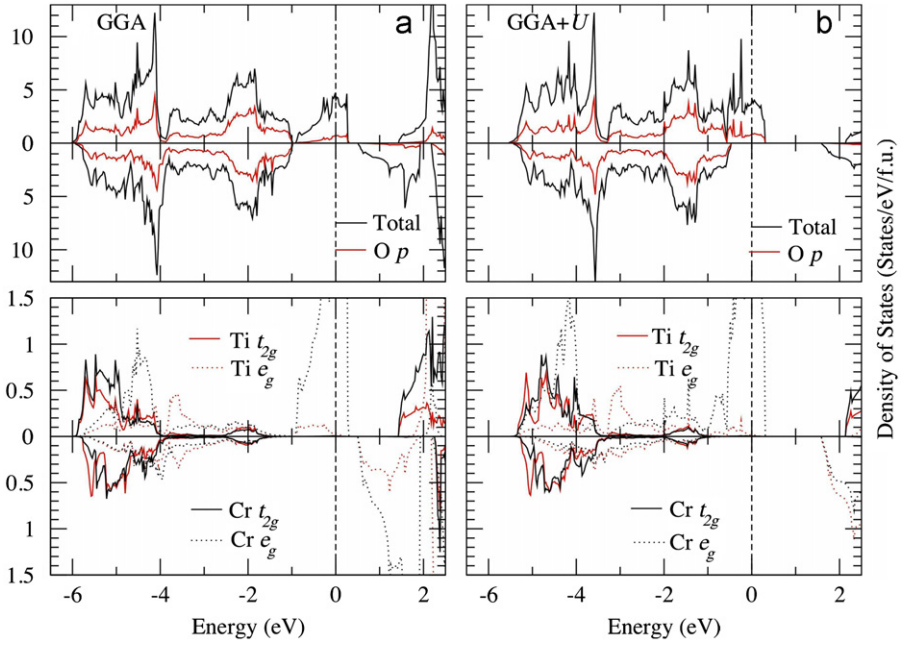

Fig. 3. (Colour online) Calculated total, spin and site decomposed density of states of Sr_2TiCrO_6: (a) GGA and (b) GGA+U(2,3).

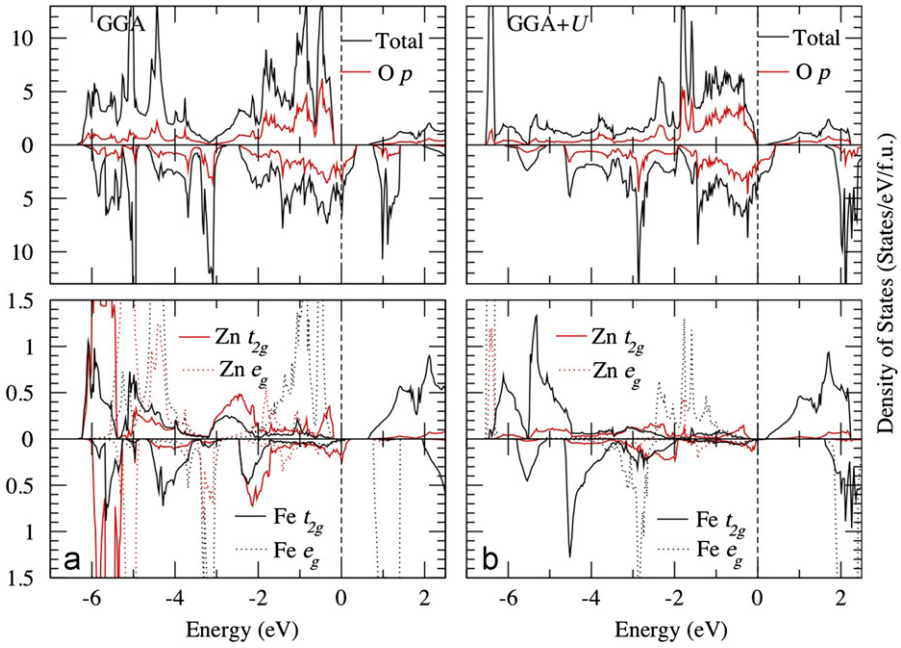

Fig. 4. (Colour online) Calculated total, spin and site decomposed density of states of Sr_2ZnFeO_6: (a) GGA and (b) GGA+U(7,5).

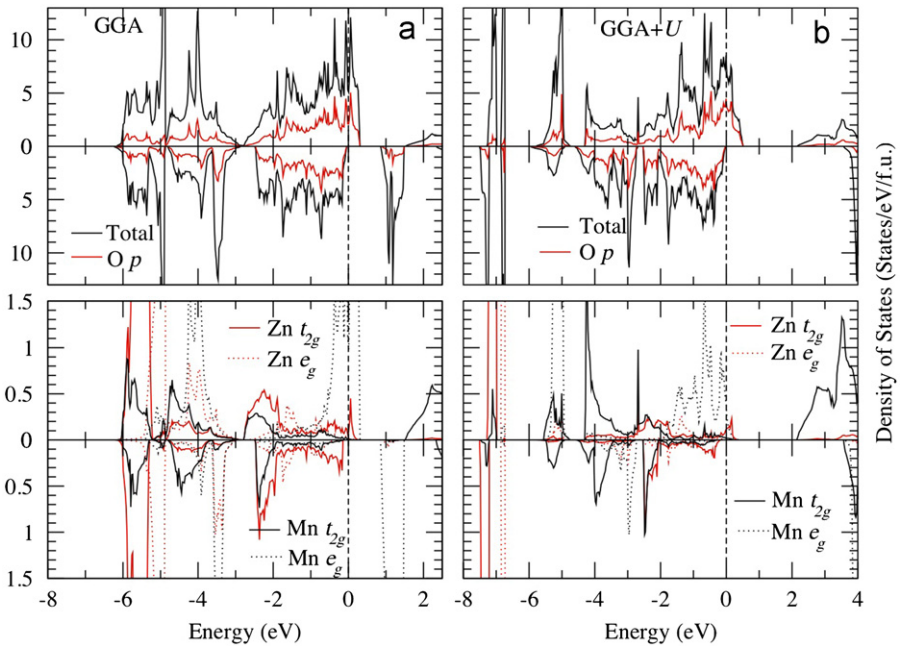

Fig. 5. (Colour online) Calculated total, spin and site decomposed density of states of Sr_2ZnMnO_6: (a) GGA and (b) GGA+U(7,5).

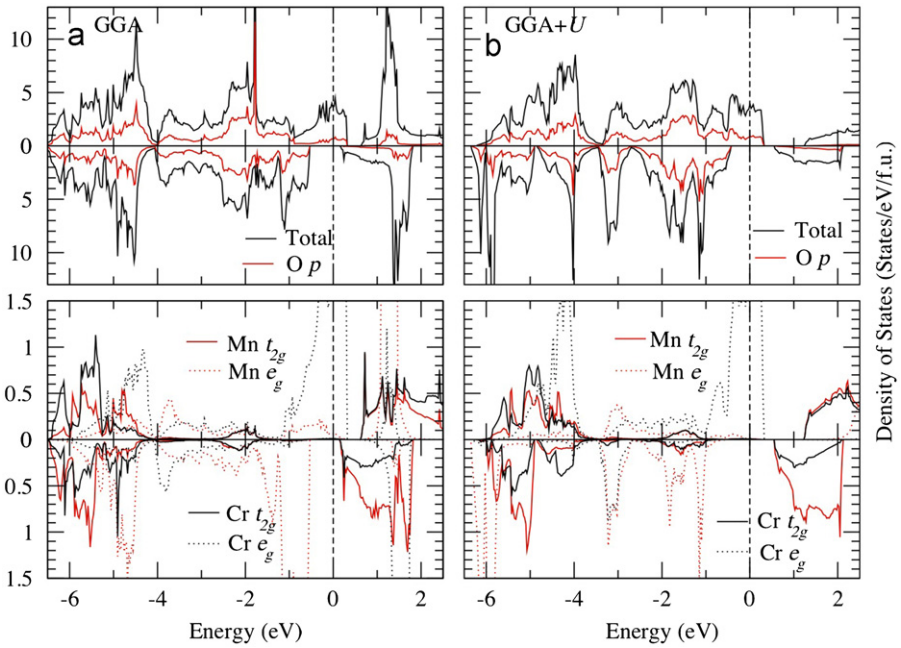

Fig. 6. (Colour online) Calculated total, spin and site decomposed density of states of Sr_2MnCrO_6: (a) GGA and (b) GGA+U(5,3).

the t_{2g} and e_g orbital indicates that the structure distortion is strong. The spin-splitting of Zn and the Zn 3d and O 2p orbital hybrid in the energy region of -6.2 eV to -0.2 eV for spin-up channel and -6.0 eV to 0.1 eV for spin-down channel causes the main HM feature. With the hybridization of the Fe t_{2g} and O 2p orbital at the conduction band, the double exchange interaction of $Fe_{t_{2g}}-O_{2p}-Zn_{t_{2g}}\downarrow$ is regarded as the main reason for the resulting FiM state. The total electron numbers of d orbital for Zn and Fe are 9.89 and 6.02, respectively. This gives the valence states of $Zn^{+0.11}(3d^{9.89})$ and $Fe^{+1.98}(3d^{6.02})$. The election configuration is $Zn^{2+}(3d^{10})$, $S=0$; $Fe^{2+}(3d^6)$, $S=2$ for Sr_2ZnFeO_6 according to the calculated electron numbers.

For Sr_2ZnMnO_6, half-metallic properties are obtained with total magnetic moment of $1.0\mu_B$ and energy gap of 0.90(3.60) eV in the GGA($+U$) calculations. The energy split of the t_{2g} and e_g orbital indicates that the structure distortion is strong. Double exchange interaction of $Mn_{e_g}-O_{2p}-Zn_{t_{2g}}\uparrow$ caused by the hybridization between the Zn 3d and O 2p orbital in the energy region of -6.1 eV to 0.3(-0.1) eV for spin up(down) channel and between the Mn 3d and O 2p orbital -6.0 eV to 0.3(0.0) eV and 1.5(0.9) eV to 2.5(1.5) eV for spin up(down) channel is regarded as the main reason for the resulting FiM state (Fig. 5). The total electron numbers of d orbital for Zn and Mn are 9.90 and 4.85, respectively. This gives the valence states of $Zn^{+0.10}(3d^{9.90})$ and $Mn^{+2.15}(3d^{4.85})$. The election configuration is $Zn^{2+}(3d^{10})$, $S=0$; $Mn^{+2}(3d^5)$, $S=1/2$ for Sr_2MnFeO_6 according to the calculated electron numbers.

For Sr_2MnCrO_6, half-metallic properties are obtained with total magnetic moment $-2.00\mu_B$ and energy gap 0.68(0.98) eV during

the GGA($+U$) calculations. Double exchange interaction of $Mn_{e_g}-O_{2p}-Cr_{e_g}\uparrow$ can result in the peaks of e_g at the Fermi level with the hybridization of Op, which is the main cause of the FiM state (Fig. 6). The total electron numbers of d orbital for Mn and Cr are 4.90 and 4.30, respectively. This gives the valence states of $Mn^{+2.10}(3d^{4.90})$ and $Cr^{+1.70}(3d^{4.30})$. The election configuration is $Mn^{+2}(3d^5)$, $S=-3/2$; $Cr^{+2}(3d^4)$, $S=1$ for Sr_2CrMnO_6 according to the calculated electron numbers.

6. Conclusions

In this paper, we present the calculated result of the $Sr_2BB'O_6$ (B,$B'=3d$ transition metal) series out of 45 combinations. The calculations are based on density functional theory (DFT) with GGA approaches. After full structural optimization and comparing the energy differences between each of 4 types of magnetic states (FM, FiM, AF and NM), there are 8 possible FM/FiM–HM stable surviving materials containing 3 FM–HM materials—Sr_2ScCrO_6, Sr_2TiCrO_6, and Sr_2ZnNiO_6—and 5 FiM–HM materials—Sr_2ScCoO_6, Sr_2TiCoO_6, Sr_2MnCrO_6, Sr_2ZnMnO_6 and Sr_2ZnFeO_6. While the on-site Coulomb interaction correction (GGA+U) is considered, there are 5 promising candidates for half-metallic (HM) materials: Sr_2ScCrO_6, Sr_2TiCrO_6, Sr_2MnCrO_6, Sr_2ZnMnO_6 and Sr_2ZnFeO_6. Double exchange interaction dominates the half-metallic characteristics of each material. We hope these results can provide more candidates and can encourage further experimental research for HM materials.

Acknowledgments

The calculations were carried out at the National Center for High-Performance Computing (NCHC) of Taiwan. The authors gratefully acknowledge resources support from the Computational Materials Research Focus Group (CMRFG) and financial supports from the Center for National Science Council (99B0320), General Education of National Normal University and National Center for High-performance Computing for computer time and facilities.

References

[1] K.-I. Kobayashi, T. Kimura, H. Sawada, K. Terakura, Y. Tokura, Nature 395 (1998) 677.
[2] J.H. Park, E. Vescovo, H.J. Kim, C. Kwon, R. Ramesh, T. Venkatesan, Nature (London) 392 (1998) 794.
[3] K.I. Kobayashi, T. Kimura, H. Sawada, K. Terakura, Y. Tokura, Nature (London) 395 (1998) 677.
[4] W.E. Pickett, J.S. Moodera, Phys. Today 54 (2001) 39.
[5] H.-T. Jeng, G.Y. Guo, Phys. Rev. B 65 (2002) 094429.
[6] K. Schwarz, J. Phys. F: Met. Phys. 16 (1986) L211.
[7] Y.K. Wang, P.H. Kee, G.Y. Guo, Phys. Rev. B 80 (2009) 224418.
[8] M.S. Park, S.K. Kwon, S.J. Toun, B.I. Min, Phys. Rev. B 59 (1999) 10018.
[9] M. Shirai, T. Ogawa, I. Kitagawa, N. Suzuki, J. Magn. Magn. Mater. 177–181 (1998) 1383.
[10] J.H. Park, S.K. Kwon, B.I. Min, Physica B 281–282 (2000) 703.
[11] F. Galasso, Inorg. Chem. 2 (1963) 482.
[12] T. Nakamura, J.H. Choy, J. Solid State Chem. 20 (1977) 233.
[13] I.V. Solovyev, J. Magn. Magn. Mater. 268 (2004) 194.
[14] Weiyu Song, Jing Wang, Zhijian Wu, Chem. Phys. Lett. 482 (2009) 246.
[15] Weiyu Song, Jing Wang, Zhijian Wu, Chem. Phys. Lett. 501 (2011) 324.
[16] S.E.A. Yousif, O.A. Yassin, J. Alloys Compd. 506 (2010) 456.
[17] V.V. Bannikov, I.R. Shein, V.L. Kozhevnikov, A.L. Ivanovskii, J. Struct. Chem. 49 (5) (2008) 781.
[18] C.M. Bonilla, et al., Physica B 398 (2007) 208.
[19] Hua Wu, Phys. Rev. B 64 (2001) 125126.
[20] C.Q. Tang, Y. Zhang, J. Dai, Solid State Commun. 133 (2005) 219.
[21] H. Kato, T. Okuda, Y. Okimoto, Y. Tomioka, Phys. Rev. B 69 (2004) 184412.
[22] Horng-Tay Jeng, G.Y. Guo, Phys. Rev. B 67 (2003) 094438.
[23] J.B. Philipp, et al., Phys. Rev. B 68 (2003) 144431.
[24] P. Hohenberg, W. Kohn, Phys. Rev. 136 (1964) B864;
W. Kohn, L.J. Sham, Phys. Rev. 140 (1965) A1133.
[25] J.P. Perdew, K. Burke, M. Ernzerhof, Phys. Rev. Lett. 77 (1996) 3865.
[26] P.E. Blöchl, Phys. Rev. B 50 (1994) 17953.
[27] G. Kresse, J. Hafner, Phys. Rev. B 48 (1993) 13115.
[28] G. Kresse, J. Furthmüller, Comput. Mater. Sci. 6 (15) (1996);
G. Kresse, J. Furthmüller, Phys. Rev. B 54 (1996) 11169.
[29] V.I. Anisimov, J. Zaanen, O.K. Andersen., Phys. Rev. B 44 (1991) 943.
[30] A.I. Lichtenstein, V.I. Anisimov, J. Zaanen., Phys. Rev. B 52 (1995) R5467.
[31] V.I. Anisimov, F. Aryasetiawan, A.I. Lichtenstein, J. Phys.: Condens. Matter 9 (1997) 767.
[32] H.-T. Jeng, G.Y. Guo, D.J. Huang, Phys. Rev. Lett. 93 (2004) 156403.
[33] X. Jiang, G.Y. Guo, Phys. Rev. B 70 (2004) 035110.
[34] I.V. Solovyev, P.H. Dederichs, V.I. Anisimov, Phys. Rev. B 50 (1994) 16861.